Layer-by-Layer Films Based on Charge Transfer Interaction of π-Conjugated Poly(dithiafulvene) and Incorporation of Gold Nanoparticles into the Films

Xiaqin Wang,[1] Kensuke Naka,[2] Chaosheng Wang,[1] Hideaki Itoh,[2] Takashi Uemura,[2] Yoshiki Chujo[2]

[1]*State Key Laboratory for Modification of Chemical Fibers and Polymer Materials, College of Material Science and Engineering, Donghua University, 1882 West Yan-an Road, Shanghai 200051, People's Republic of China*
[2]*Department of Polymer Chemistry, Graduate School of Engineering, Kyoto University, Katsura, Nishikyo-ku, Kyoto 615-8510, Japan*

Received 22 August 2005; accepted 11 January 2006
DOI 10.1002/app.24638
Published online in Wiley InterScience (www.interscience.wiley.com).

ABSTRACT: Layer-by-layer (LBL) self-assembled ultrathin films were prepared via consecutively alternating immersion of substrates into solutions of electron donor, poly(dithiafulvene) (PDF), and electron acceptor, poly(hexanyl viologen) (6-VP). The charge transfer (CT) interaction formed at solid–liquid interfaces between the backbones of the electron acceptor and donor polymers was the driving force of the alternative deposition. The sandwich heterostructure of the LBL film led to electrical anisotropy in the directions parallel and perpendicular to the film surfaces. Incorporation of gold nanoparticles into the LBL films was investigated by reducing gold ions with the PDF layers already deposited on the film surfaces, or depositing PDF-protected gold colloidal solution as the electron donor layers directly. The influence of the gold nanoparticles on the electrical anisotropy of the LBL films was also illustrated in this research. © 2006 Wiley Periodicals, Inc. J Appl Polym Sci 103: 1608–1615, 2007

Key words: layer-by-layer self-assembled film; poly(dithiafulvene); poly(hexanyl viologen); gold nanoparticles; charge transfer interaction; electrical anisotropy

INTRODUCTION

Self-assembled LBL films have been intensively investigated in recent years because of their simplicity, since Gero and colleagues[1,2] established the method for preparing multilayer ultrathin films by the consecutive deposition of oppositely charged polyelectrolytes from dilute aqueous solution onto charged substrates. The most substantial advantages of the LBL self-assembly are a molecular-level control over film thickness and a supramolecular architecture of polyelectrolyte layers, where the macroscopic properties of the LBL films are controlled by the microscopic structures.[3] Forces between the layers are primarily electrostatic interaction and covalent bonding, but they can also involve hydrogen bonding, π–π interaction, and coordination bonding of monomeric or polymeric ligands with transition metal ions.[4,5] A relatively weaker charge transfer (CT) interaction as the driving force of the LBL self-assembly was recently used to prepare ultrathin films.[6–9] Incorporation of noble metal nanoparticles into the LBL films consisting of π-conjugated conducting polymers presents promising materials for both catalytic applications, in which conducting polymer beds with catalyst nanoparticles gathering close to the film surfaces provide optimum catalytic situations, and nanotechnological fabrication. To date, anisotropically conductive ultrathin films via self-assembly of conjugated polymers based on CT interaction and incorporation of nanoparticles into host LBL films involving conjugated conducting polymers have not been reported. High conductivity difference in different directions is desirous and significant for application of the LBL films in electronic devices, although low interpenetration of polymer chains is still possible between the stratified layers.

Electron donation from a π-conjugated poly(dithiafulvene) (PDF) to metal ions also generated metal (Pd, Au, Pt) nanoparticles of 5–6-nm size, with the resulting oxidized PDF protecting the metal nanoparticles.[10,11] We have recently reported an initial study on LBL films, in which CT interaction promoted the

Correspondence to: X. Wang (xqwang@dhu.edu.cn).
Contract grant sponsor: National Natural Science Foundation of China (NSFC); contract grant number: 50403004.
Contract grant sponsor: Ministry of Education, Culture, Sports, Science, and Technology, Government of Japan; contract grant number: 16310086.
Contract grant sponsor: COE for a United Approach to New Material Science (21st Century COE Program).
Contract grant sponsor: Shanghai Nanotechnology Promotion Center; contract grant number: 0452NM079.
Contract grant sponsor: Scientific Research Foundation for the Returned Overseas Chinese Scholars, State Education Ministry.

self-assembly between polymeric backbones of PDF and poly(hexanyl viologen) (6-VP) as an electron acceptor polymer.[12] Huge electrical anisotropy as high as 2 orders of magnitude was observed due to the periodic layers of the high content of CT complexes contained in the LBL heterostructure, more than 10 times the reported value for a poly(cyclopentadithiophene) based LBL film via electrostatic interaction.[13] In the present work, a detailed investigation was made on fabrication of the anisotropically conductive LBL films. We describe new approaches to the generation of macroscopic metal surfaces in the LBL films from self-assembly of colloidal gold nanoparticles and immobilization of gold nanoparticles via reduction of gold ions by the PDF layers that were already deposited on the LBL films. We also studied the influence of the incorporated gold nanoparticles on the film structures, morphologies, and electrical anisotropy.

EXPERIMENTAL

Materials

Unless stated otherwise, all reagents and chemicals were obtained from commercial sources and used without further purification. PDF was synthesized by the cycloaddition polymerization of bis(aldothioketene) with its alkynethiol tautomer derived from 1,4-diethynylbenzene according to our previous reports.[14,15] The number-average molecular weight (M_n) of PDF was 3400, determined by ^{1}H NMR. Comparison of the intensities of the absorption of the dithiafulvene protons in the repeating units with those of the absorptions of the terminal thioamide protons results in the estimation of number-average degree of polymerization. 6-VP was prepared from 1,6-dibromohexane and 4,4′-bipyridyl as reported,[16] and its counterions were transformed to hexafluorophosphate (PF_6^-). The M_n of 6-VP was 2400 determined by ^{1}H NMR with a similar method to that used for PDF. The chemical structures of PDF and 6-VP are shown in Chart 1.

Preparation of LBL films

Indium-doped tin oxide (ITO) glass substrates were washed with *n*-hexane and sonicated in a 70 wt% aqueous solution of nitric acid for 30 min. Then the substrates were cleaned with distilled water and methanol, and dried overnight in an oven at 100°C. Surface modification of the clean ITO glass substrates was performed before fabrication of LBL films. At first, a negatively charged ITO substrate was immersed into a 5.0 wt% aqueous solution of poly(diallyldimethylammonium chloride) for 30 min to introduce positive charges onto the substrate surface.[17] The substrate was then washed with a large amount of distilled water and dried completely in a vacuum. This step was repeated to improve the adsorption of the cationic polymer. Then the substrate was immersed into a 1.0 wt% aqueous solution of poly(sodium 4-styrenesulfonate) (PSSNa) for 30 min to induce stable charge reversal,[18,19] as shown in Figure 1. The substrate was washed with a large amount of distilled water and dried in a vacuum again. The adsorbed polymers on the insulated side of the ITO glass substrate were wiped off by Kimwipes wipers (Kimberly-Clark Corp., USA) with distilled water to prevent the insulated side from adsorbing the polymers. The modified ITO glass slide with negatively charged surface was used as the substrate for repeated adsorption of the positively charged electron acceptor, i.e., 6-VP, and the π-conjugated electron donor, i.e., PDF, subsequently.

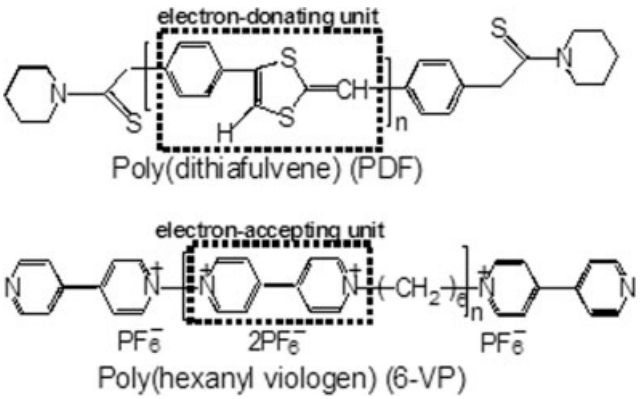

Chart 1 Chemical Structures of the Electron Donor and Acceptor Polymers.

The alternative deposition of 6-VP and PDF was carried out as follows (Fig. 1). At first, the modified substrate was immersed in a 1.0 wt% dimethylsulfoxide (DMSO) solution of 6-VP for 20 min and washed with DMSO carefully to remove unabsorbed 6-VP. The insulated side of the substrate was wiped with DMSO to avoid 6-VP adsorbing on this side. After being dried in a vacuum, the substrate was dipped into a 0.5 wt% DMSO solution of PDF for 15 min. The washing and drying steps were the same as those following the adsorption of 6-VP. The immersion step of PDF was repeated to ensure complete adsorption of PDF. In fact, adsorption of PDF was hardly recognized after the second dipping process compared with the first dipping by UV-vis absorption measurements. Multilayer films were obtained by repeating the alternating immersion steps in the 6-VP and PDF solutions as described above. Molecular recognition by CT interaction between the donor and acceptor layers permits the LBL self-assembly, as shown in the inset of Figure 1. The backbones of the π-conjugated PDF are simplified into bold curves, and the bead-like units scattered on the thin curves represent the elec-

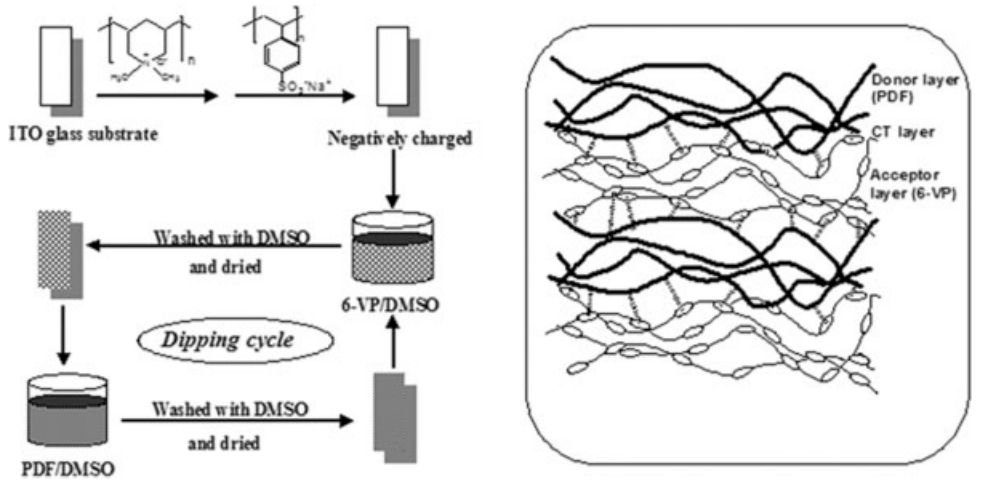

Figure 1 Experimental procedures for the surface modification of an ITO glass substrate and subsequent LBL self-assembly of 6-VP and PDF on the substrate.

tron acceptor sections in 6-VP backbones. CT complexes formed between PDF and 6-VP are depicted with broken lines. One layer of PDF and one layer of 6-VP are called one bilayer in this work.

Incorporation of gold nanoparticles into the LBL films

Two strategies were employed to incorporate gold nanoparticles into the LBL films. One strategy is that after a bilayer of 6-VP and PDF was deposited on a modified ITO glass substrate as described above, the top PDF layer was further oxidized by a 0.99 wt% aqueous solution of hydrogen tetrachloroaurate (III) tetrahydrate chloroauric acid ($HAuCl_4{\cdot}4H_2O$) for 12 h and the gold ions in the solution were reduced into the metallic form concurrently (Fig. 2). After the oxidation, the LBL film was washed with distilled water three times to remove the ions adsorbed on the film surface and dried in a vacuum. In the next dipping cycle, another bilayer of 6-VP and PDF was self-assembled on the film, and then the PDF layer was oxidized by the $HAuCl_4$ solution. The LBL film with a monolayer of gold nanoparticles interposed on each PDF layer was produced by repeating the dipping cycle.

The other strategy is that the fabrication procedure of the LBL film was the same as described above except that a PDF-protected gold colloidal solution was used to replace the aforementioned 0.5 wt% DMSO solution of PDF for the alternative deposition cycles, as shown in Figure 3. A PDF-protected gold colloidal solution was prepared by a slightly modified method as reported by our group.[10] PDF (5.0 mg, 2.6×10^{-2} mmol by repeating units) was dissolved into a DMSO solution (10 ml) of $HAuCl_4{\cdot}4H_2O$ (0.5 mg, 1.2×10^{-3} mmol). The PDF-protected gold nanoparticles were used as an electron donor in the dipping cycles after the colloidal solution was stirred vigorously for 1 week at room temperature. The multilayer film was obtained

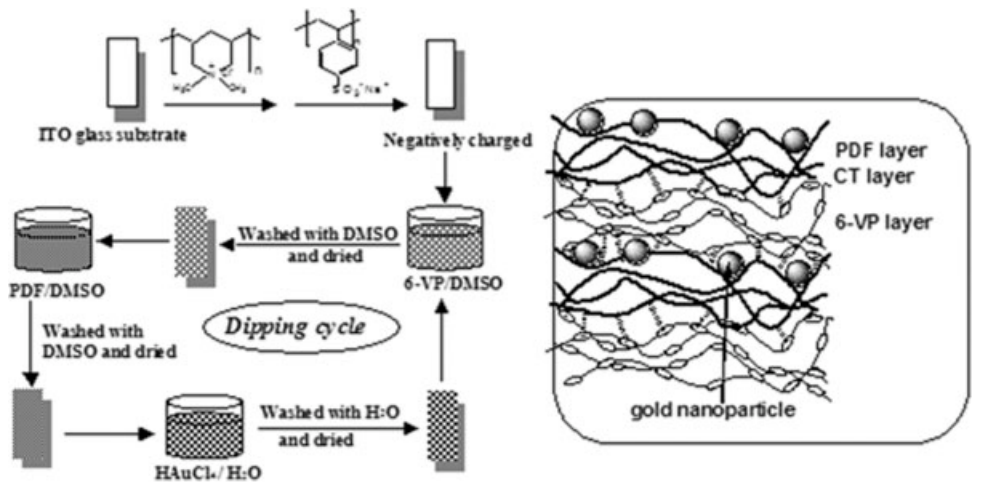

Figure 2 Experimental procedures for the immobilization of gold nanoparticles by reducing gold ions with PDF layers.

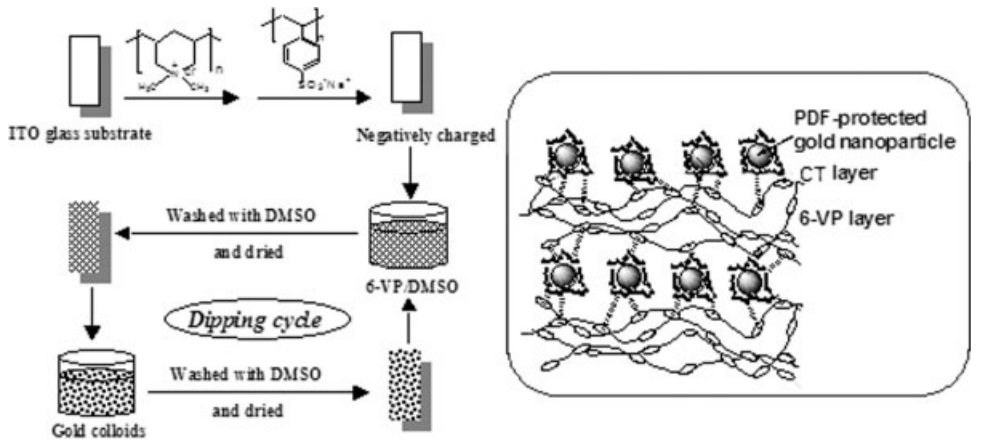

Figure 3 Experimental procedures for the introduction of gold nanoparticles via direct deposition of a PDF-protected gold colloidal solution.

by repeating the alternating immersion steps in the 6-VP and PDF-protected gold colloidal solutions.

Characterization

^{1}H NMR spectra were obtained with a JEOL JNM-EX270 spectrometer (270 MHz for ^{1}H NMR) in DMSO-*d*. UV-vis absorption spectra of the solutions and multilayer films were recorded using a Jasco-530 spectrophotometer. Backgrounds of the negatively modified substrates were subtracted from all spectra of the multilayer films. ESR spectra were recorded at X-band frequency with a JEOL JES-RE spectrometer in quartz capillaries of 4 mm internal diameter. Oriented electrical conductivities of the multilayer films were measured at room temperature by a two-probe technique using a Keithley model 236 Source measurement unit (Keithley Instruments Inc., Cleveland, OH) with a home-built sample holder. For the conductivity in the direction parallel to the film surface, two thin Pt wire leads were contacted at the surface of the film with carbon paste. For the perpendicular conductivity, one Pt wire lead was contacted at the surface of the film and the other Pt wire lead was contacted at the unmodified area of the ITO glass surface. Cyclic voltammograms of the LBL films were measured in acetonitrile solutions of 0.1 M $[NEt_4]BF_4$ at 300 mV s^{-1} with a BAS CV-50 W Electrochemical Analyzer. Scanning electron microscopy (SEM) was performed using a JEOL JNM-5310/LV system operated at an accelerating voltage of 20–25 kV. Transmission electron microscopy (TEM) images were taken on a JEOL JEM-100SX operated at an accelerating voltage of 100 kV.

RESULTS AND DISCUSSION

CT complexation of PDF and 6-VP

A characteristic maximal absorption at 600 nm for a soluble CT complex appeared in the UV-vis absorption spectrum for the DMSO solution of PDF and methyl viologen dihexafluorophosphate as an electron-accepting unit of 6-VP. Admixtures of PDF and 6-VP in DMSO instantaneously produced green precipitates, which are the diagnostic of CT interaction between two kinds of the polymers. The ESR spectrum of the precipitates consisted of two types of signals. A sharp signal ($g = 2.005$) was assigned to the anion radical of the viologen unit.[20] A broad singlet line ($g = 2.011$) is almost the same as that of the ESR signal of the TTF-TCNQ complex.[14] The green precipitates consisting of PDF and 6-VP were prepared by accurate addition of different molar ratios of PDF and 6-VP in DMSO. As shown in Table I, elemental analyses revealed that the molar ratios of the two polymers in the CT complexes were independent of the various distinct initial feed molar ratios of the repeating units in the two polymers. VM and DF denote the repeating units in 6-VP and PDF, respectively.

Preparation of LBL films

Based on the above results that the CT complex was formed between PDF and 6-VP, LBL films were prepared via consecutively alternating immersion of the modified substrates into DMSO solutions of PDF and 6-VP, respectively. The overlaid UV-vis absorption spectra of a LBL deposition process of PDF and 6-VP

TABLE I
CT Complexes of PDF with 6-VP in DMSO

[VM]/[DF]	Yield (%)	[VM]/[DF] in the CT complexes
0.07	20	—
0.11	54	0.22
0.18	58	0.19
0.29	36	0.24
0.43	34	0.15
1.0	14	0.17

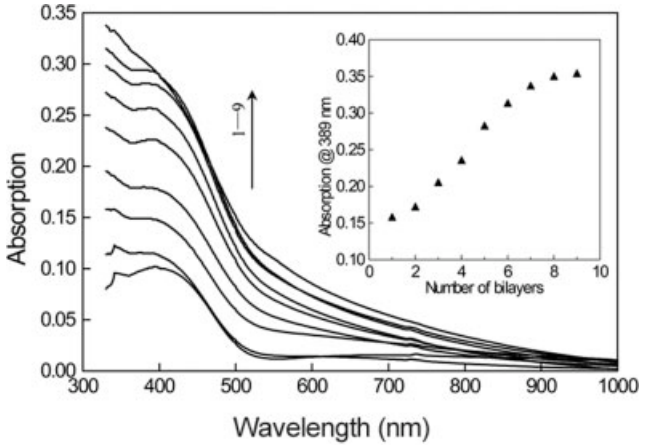

Figure 4 UV-vis absorption spectra of 1–9 bilayers of 6-VP and PDF deposited on an ITO glass substrate. Inset shows the absorption at 389 nm increases with the number of bilayers.

for a nine-bilayer film are presented in Figure 4. The absorption maxima at 389 nm derived from PDF increase with the bilayers deposited on the film, as shown in the inset. The absorption below 550 nm is mainly from the accumulative absorption of PDF and 6-VP, and the broad absorption band up to 1000 nm is ascribed to the CT complexes formed at the solid–liquid interfaces between the electron donor and acceptor polymers. The absorbance of the CT complex layers increased with the number of the deposited bilayers.

The total thickness increase with the number of the bilayers of 6-VP and PDF, and the thickness of each PDF layer, are shown in Figure 5. The molar absorption coefficient at 389 nm of the DF unit in PDF ($\varepsilon = 3.28 \times 10^3\ M^{-1}\ cm^{-1}$) was used for calculation of the PDF layer thickness, assuming that the density of the bulk film was 1.0 g/cm^3. The thickness of the first PDF layer was three times that of the others. This phenomenon can be explained by a larger amount of 6-VP adsorption on the PSSNa layer from the pretreatment of the glass substrate than on the subsequent PDF layers as electrostatic interaction between PSSNa and 6-VP is relatively stronger than the CT interaction between 6-VP and PDF. A linear relationship was observed between the total thickness and the number of deposited bilayers until the seventh bilayer, which indicates the deposition process in all cases is reproducible from layer to layer. The average thickness of each PDF layer except the first one was 24 nm. Relatively thicker layers might be produced by the existence of a greater fraction of PDF segments in loops and tails due to lower levels of intrasegmental repulsion of PDF.[21] Termination of growth after nine bilayers was observed due to the relatively weak interaction between the donor and acceptor polymers. A similar phenomenon occurred when we used hydrogen bonding as the driving force for other LBL self-assemblies.

Oriented electrical conductivity measurement of the nine-bilayer film provided an electrical conductivity of 1.4×10^{-5} S cm^{-1} in the direction perpendicular to the film surface. However, the conductivity rose to 3.8×10^{-3} S cm^{-1} in the direction parallel to the film surface, more than 2 orders of magnitude greater than that in the direction perpendicular to the film surface. Pure 6-VP showed a conductivity of 9.4×10^{-6} S cm^{-1}, slightly lower than the perpendicular conductivity of the nine-bilayer film. A small amount of PDF molecular interpenetration in the film occurred, which caused the perpendicular conductivity higher than the conductivity of 6-VP, whereas the parallel conductivity of the film was of the same order of magnitude as that of doped PDF. This result indicates that the conduction along the polymer layer is scarcely modified by alternating insulating layers. The electrical anisotropy ensured the formation of the LBL heterostructure multilayer film. The LBL heterostructure in the multilayer film was further supported by cyclic voltammogram (CV) measurements. An oxidation peak at 0.84 V vs Ag/AgCl appeared for the CT complex of PDF with 6-VP, shifted from 0.61 V vs Ag/AgCl for uncomplexed PDF originating from electron-withdrawing effect of 6-VP. But a series of the LBL films on the ITO glass substrates bearing 1, 2,

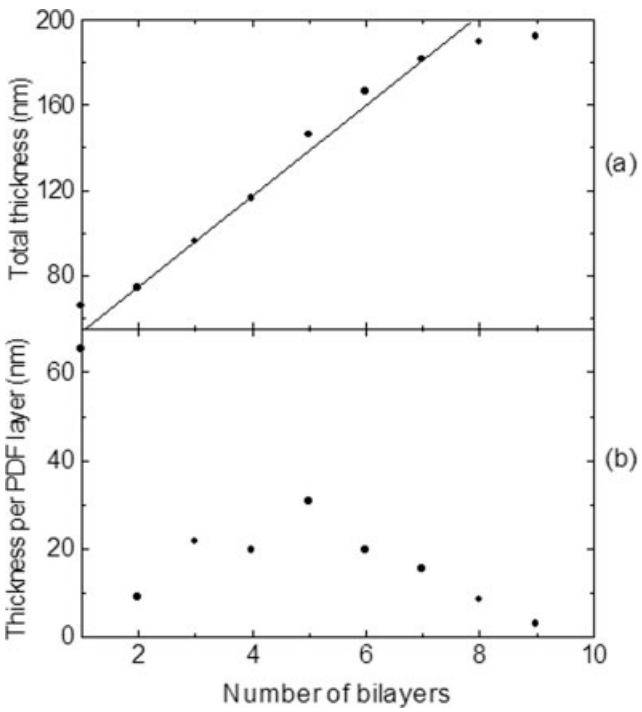

Figure 5 Dependence of (a) total thickness and (b) thickness per PDF layer on the number of bilayers. PDF layer thickness was estimated from UV-vis absorption at 389 nm.

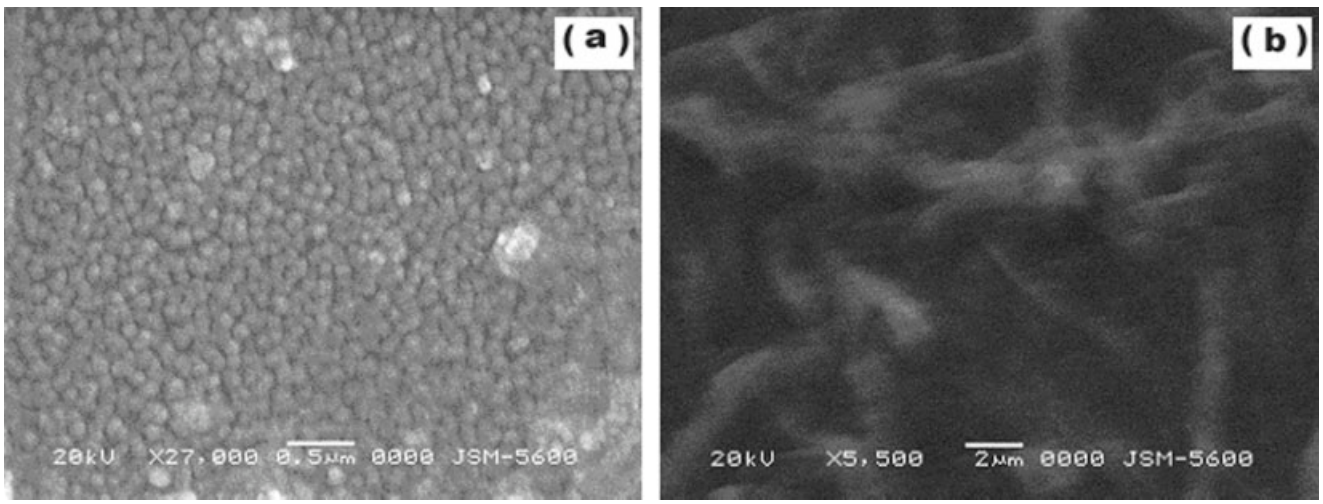

Figure 6 SEM images of the top PDF layer on a two-bilayer film (a) after, and (b) before the reduction by gold ions.

3, 4, 5, 8, and 9 bilayers, respectively, exhibited no oxidation peaks. This result is consistent with the electrical properties of the multilayer films. In the direction perpendicular to the film surface, electron transfer was hindered compared with that in the direction parallel to the film surface due to the sandwich heterostructures of the multilayer films, and therefore a redox reaction did not occur during CV measurements.

Integration of gold nanoparticles into the LBL films by reduction of the gold ions with the PDF layers

Two strategies were studied to introduce gold nanoparticles into the LBL films. The first strategy is that gold ions were reduced by the PDF layer already deposited on the film surface and the resulting gold nanoparticles were then tethered by the oxidized PDF on the film surface. The interaction between the PDF layer on a two-bilayer film and Au^{3+} in the 0.99 wt% $HAuCl_4$ aqueous solution was elucidated by a 6.6% absorption decrease of the maximal absorption of the $HAuCl_4$ solution at 292 nm in the UV-vis absorption spectra. The SEM image in Figure 6(a) showed that the gold nanoparticles with size of about 100 nm packed densely on the film surface with a coverage density of 1.75×10^{-10} mg (8.88×10^{-13} mmol)/μm^2 estimated from the absorption decrease at 292 nm of the $HAuCl_4$ solution. No overlapping of two or more gold nanoparticles occurred. In contrast, nothing but a smooth film surface was observed before the oxidation of the two-bilayer film [Fig. 6(b)]. During the deposition process of a five-bilayer film, each PDF layer was oxidized by the gold ions at the end of each dipping cycle, and finally the film turned out to be light red. Weak surface plasmon absorption at 530–580 nm due to gold nanoparticles with smaller sizes was observed in the UV-vis absorption spectra, as shown in Figure 7. However, most of the gold particles made no contribution to the maximal plasmon absorption due to their large size. These results illustrated that the gold nanoparticles were generated by reduction with the PDF layers and deposited on the PDF layers simultaneously. The partially oxidized PDF layers immobilized the gold nanoparticles efficiently via Au—S bonds, and were still capable of forming CT complex with 6-VP in the next dipping cycle.

The electrical conductivity of the five-bilayer film with gold nanoparticle arrays on the top was 1.1×10^{-4} S cm^{-1} in the direction parallel to the film surface and 6.8×10^{-6} S cm^{-1} in the direction perpendicular to the film surface. The conductivity of the gold nanoparticle arrays was 2.8×10^{-9} S cm^{-1} for an ultrathin film of 2.4-nm diameter gold nanoparticles

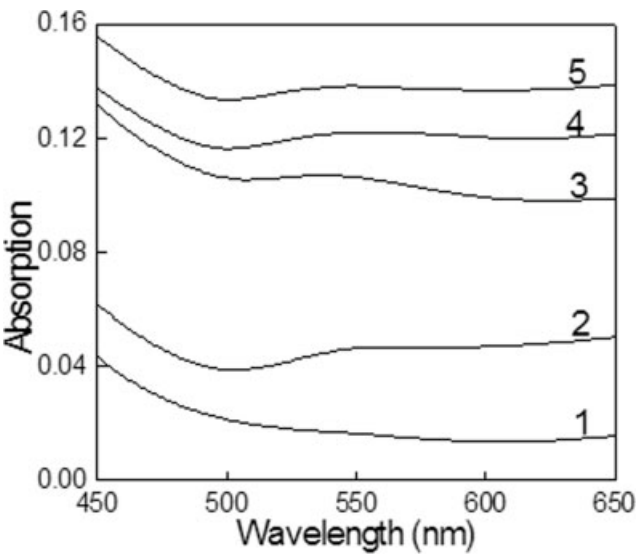

Figure 7 UV-vis absorption spectra of 1–5 bilayers of 6-VP and PDF with the gold nanoparticles interposed on each PDF layer.

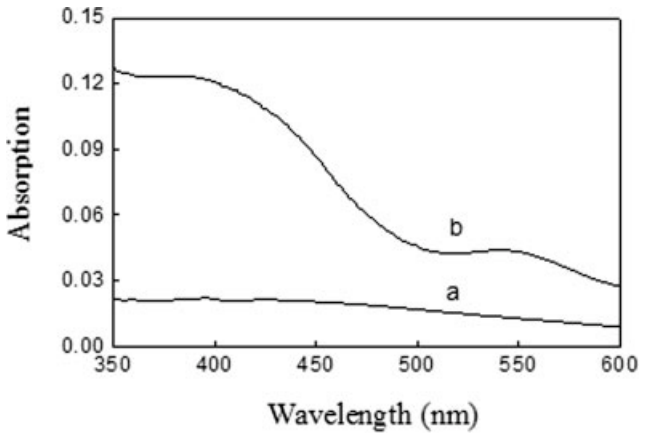

Figure 8 UV-vis absorption spectra (a) before, and (b) after the deposition of the gold colloidal solution on the first 6-VP layer.

spaced by 1,16-hexadecanethiol.[22] So far none of particle arrays has approached the conductivity of pure gold (4.2×10^5 S cm^{-1}).[23] The crosslinking of the gold nanoparticles by the conducting PDF layer played a crucial role for the increased conductivity of the gold nanoparticle arrays loaded on the five-bilayer film. The large sizes of the gold nanoparticles and the activated electron hopping at the interfaces between the metallic gold and PDF molecules might produce changes in the electrical properties of the LBL film as well. The parallel conductivity of the film decreased by over 30 times due to the loading of the gold nanoparticles on the PDF layers.

LBL films by direct deposition of a PDF-modified gold colloidal solution

Based on our previous work, reduction of $HAuCl_4$ by PDF led to gold nanoparticles of narrow size distribution and high dispersity with the resulting oxidized PDF protecting the gold nanoparticles in DMSO.[10] The uniformly oxidized PDF could still undergo a further oxidation during CV measurement,[11] which means PDF was partially oxidized and able to form CT complexes with electron acceptors. Accordingly, another strategy of incorporating gold nanoparticles into the LBL films was established, in which an electroactive PDF-protected gold colloidal solution was used to substitute the PDF solution in alternative deposition as the electron donor layers. The average size of the gold nanoparticles in the colloidal solution was 10 nm estimated from TEM. Comparison of the UV-vis spectra before and after the treatment with the PDF-protected gold colloidal solution on the first 6-VP layer already deposited on the modified substrate revealed that the maximal absorption at 550 nm for the surface plasmon resonance of the gold nanoparticles along with the characteristic absorption maximum at 389 nm for PDF appeared after the treatment, indicating the deposition of the PDF-protected gold colloidal layer on the 6-VP layer (Fig. 8). A two-bilayer film was obtained by repeating the dipping cycle. The two-bilayer film showed a pale red color, corresponding to the increased surface plasmon resonance of the gold nanoparticles. A homogeneous distribution of the gold nanoparticles in the LBL film occurred when the preformed PDF-protected gold colloidal solution was deposited on the 6-VP layers by CT interaction (Fig. 9). However, the density of gold nanoparticles was much lower than that in Figure 6.

CONCLUSIONS

The LBL self-assembled ultrathin films with controlled thickness were successfully prepared via the adoption of a simple approach of immersing the modified ITO glass substrate alternatively in the 6-VP

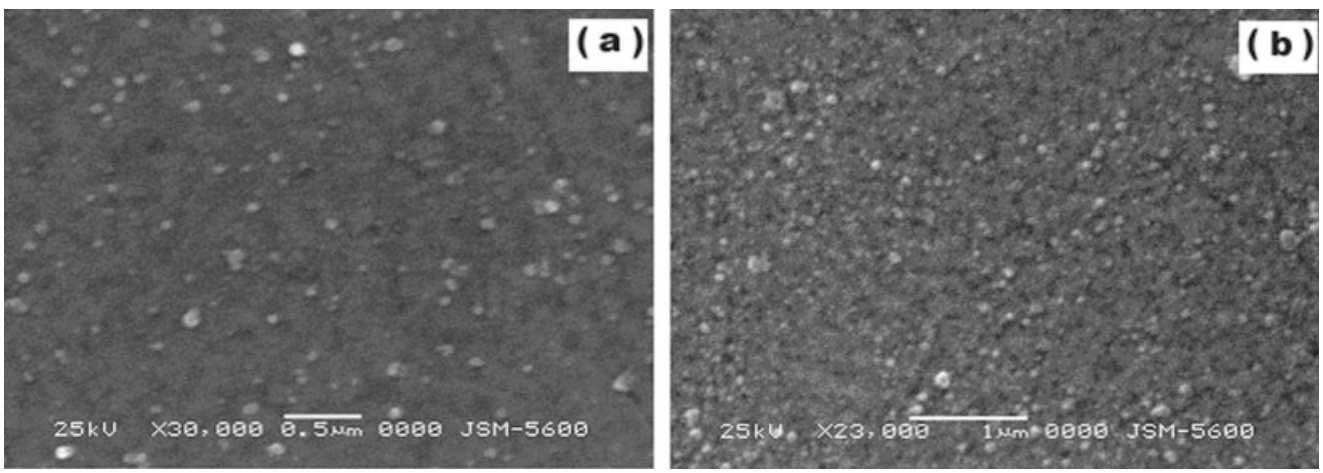

Figure 9 SEM images of gold nanoparticles immobilized in a LBL film bearing (a) one bilayer, and (b) two bilayers of acceptor and donor polymers.

and PDF solutions. CT interaction formed between the polymer backbones of the electron acceptor and donor in the ultrathin films was the driving force for the LBL self-assembly. The nine-bilayer LBL film showed a high conductivity anisotropy with the values of 3.8×10^{-3} S cm^{-1} and 1.4×10^{-5} S cm^{-1} for the parallel and perpendicular conductivities, respectively, as a result of the heterostructure of the LBL film although intermixing occurred on a molecular level. Introduction of the gold nanoparticles into the LBL films was performed by oxidizing the PDF layers in the LBL films with the $HAuCl_4$ solution, and direct deposition of the PDF-protected gold colloidal solution. Both of them ensured good compatibility of the gold nanoparticles with the host LBL films. The inclusion methods of the gold nanoparticles into the LBL films are also applicable to other metal or semiconductor nanoparticles, such as Pt, Pd, and PbS.[11,24]

References

1. Decher, G.; Hong, J. D.; Schmitt, J. Thin Solid Films 1992, 210/211, 831.
2. Lvov, Y.; Decher, G.; Moehwald, H. Langmuir 1993, 9, 481.
3. Gero, D.; Schmitt, J. Prog. Colloid Polym Sci 1992, 89, 160.
4. Bell, C. M.; Arendt, M. F.; Gomez, L.; Schmehl, R. H.; Mallouk, T. E. J Am Chem Soc 1994, 116, 8374.
5. Kim, J.; Wang, H. C.; Kumar, J.; Tripathy, S. K.; Chittibabu, K. G.; Cazeca, M. J.; Kim, W. Chem Mater 1999, 11, 2250.
6. Shimazaki, Y.; Mitsuishi, M.; Ito, S.; Yamamoto, M. Langmuir 1997, 13, 1385.
7. Shimazaki, Y.; Mitsuishi, M.; Ito, S.; Yamamoto, M. Langmuir 1998, 14, 2768.
8. Shimazaki, Y.; Ito, S. Langmuir 2000, 16, 9478.
9. Shimazaki, Y.; Nakamura, R.; Ito, S.; Yamamoto, M. Langmuir 2001, 17, 953.
10. Zhou, Y.; Itoh, H.; Uemura, T.; Naka, K.; Chujo, Y. Chem Commun 2001, 613.
11. Zhou, Y.; Itoh, H.; Uemura, T.; Naka, K.; Chujo, Y. Langmuir 2002, 18, 277.
12. Wang, X.; Naka, K.; Itoh, H.; Uemura, T.; Chujo, Y. Macromolecules 2003, 36, 533.
13. Berlin, A.; Zotti, G. Macromol Rapid Commun 2000, 21, 301.
14. Naka, K.; Uemura, T.; Chujo, Y. Polym J 2000, 32, 435.
15. Naka, K.; Uemura, T.; Chujo, Y. Macromolecules 1998, 31, 7570.
16. Harada, A.; Adachi, H.; Kawaguchi, Y.; Okada, M.; Kamachi, M. Polym J 1996, 28, 159.
17. Li, D.; Jiang, Y.; Wu, Z.; Chen, X.; Li, Y. Thin Solid Films 2000, 360, 24.
18. Dubas, S. T.; Schlenoff, J. B. Macromolecules 1999, 32, 8153.
19. Sukhorukov, G. B.; Donath, E.; Lichtenfeld, H.; Knippel, E.; Knippel, M.; Budde, A.; Öhwald, H. M. Colloids Surf A: Physicochem Eng Aspects 1998, 137, 253.
20. Ranjit, K. T.; Kevan, L. J Phys Chem B 2002, 106, 1104.
21. Ferreira, M.; Rubner, M. F. Macromolecules 1995, 28, 7107.
22. Terrill, R. H.; Postlewaite, T. A.; Chen, C. H.; Poon, C. D.; Terzis, A.; Chen, A.; Hutchison, J. E.; Clark, M. R.; Wignall, G.; Londono, J. D.; Superfine, Flavo, R. M.; Johnson, C. S., Jr.; Samulski, E. T.; Murray, R. W. J Am Chem Soc 1995, 117, 12537.
23. Musick, M. D.; Keating, C. D.; Keefe, M. H.; Botsko, S. L.; Natan, M. J. Chem Mater 1997, 9, 1499.
24. Zhou, Y.; Itoh, H.; Uemura, T.; Naka, K.; Chujo, Y. Langmuir 2002, 18, 5287.